Quaternion Analysis of Transient Phenomena of Motor-Generator*)

Kazuo NAKAMURA, Yifan ZHANG[1)], Takumi ONCHI, Hiroshi IDEI, Makoto HASEGAWA, Kazutoshi TOKUNAGA, Kazuaki HANADA, Takeshi IDO, Ryuya IKEZOE, Hirotaka CHIKARAISHI[2)], Osamu MITARAI[3)], Shoji KAWASAKI, Aki HIGASHIJIMA, Takahiro NAGATA and Shun SHIMABUKURO

Research Institute for Applied Mechanics, Kyushu University, 6-1 Kasugakoen, Kasuga 816-8580, Japan
[1)]*Interdisciplinary Graduate School of Engineering Sciences, Kyushu University, 6-1 Kasugakoen, Kasuga 816-8580, Japan*
[2)]*National Institute for Fusion Science, 322-6 Oroshi-cho, Toki 509-5292, Japan*
[3)]*Tokai University, Kumamoto 862-8652, Japan*

(Received 9 January 2023 / Accepted 22 March 2023)

A motor-generator slowly converts low electrical power to the large rotating energy of the induction motor, which is then converted to the higher electrical power of the synchronous generator through a pulse. Such a cycle is repeated in a tokamak plasma experiment. In the transient phase at the start of the synchronous generator, high transient voltage appears in the armature windings repeatedly. Due to the repeatability, it is imperative to estimate the high voltage and control it so that the maximum voltage is kept under a tolerable value. A quaternion is a four-dimensional hypercomplex number that is good at describing three-dimensional rotation. Utilizing the quaternion capability, a three-phase motor-generator is analyzed using three-dimensional rotation. The mechanical rotation was anlyzed by the rotation quaternion. The salient pole-type rotating field can be manipulated by direct-quadrature conversion even in quaternion analysis. The rotating dynamics and electrical phenomena of a motor-generator can be analyzed by considering the quaternion power from the motor-generator and the electrical load for plasma control.

Keywords: quaternion analysis, three-phase to three-phase, transient phenomena, motor-generator, regenerative mode

DOI: 10.1585/pfr.18.2405035

1. Introduction

A motor-generator converts low electrical power to the large rotating energy of the induction motor over a long time period (300 s) and the large rotating energy is converted to the higher electrical power of the synchronous generator, which controls power supplies for a short time (3 s). Such a cycle is repeated every five minutes in a tokamak plasma experiment.

In the transient phase at the start of the synchronous generator, high transient voltage appears in the armature windings repeatedly. Due to the repeatability, it is imperative to estimate the high voltage and control it so that the maximum voltage is kept under a tolerable value.

The quaternion is a four-dimensional hypercomplex number that is good at describing three-dimensional rotation, such as that seen in three-dimensional graphics and simulation programming theory. Utilizing the quaternion capability, the three-phase motor-generator was analyzed using three-dimensional rotation as an alternative to transforming to two-dimensional rotation in alpha-beta coordinates [1]. The mechanical rotation can be analyzed by a rotation quaternion instead of a rotation matrix. The salient pole-type rotating field can be manipulated by direct-quadrature conversion even in quaternion analysis.

The rotating dynamics and electrical phenomena of a motor-generator can be analyzed considering the quaternion power from the motor-generator and the electrical load for plasma control. Since the quaternion can be differentiated in time as well as rotated in space [2], it is utilized to analyze transient phenomena in the rise-up and rise-down of the induction motor and the synchronous generator. The quaternion characteristics will be utilized to analyze a motor-generator in more detail.

2. Quaternion and the Differentiation

The quaternion is a four-dimensional hypercomplex number, which is extended from a complex number [3] to express three-phase AC voltage (Alternating voltage) in three dimensions:

author's e-mail: nakamura@triam.kyushu-u.ac.jp

*) This article is based on the presentation at the 31st International Toki Conference on Plasma and Fusion Research (ITC31).

$$\boldsymbol{q} = a + \hat{v} = a + (\hat{i}v_{\rm x} + \hat{j}v_{\rm y} + \hat{k}v_{\rm z}), \tag{1}$$

$$\hat{i}^2 = \hat{j}^2 = \hat{k}^2 = -1, \tag{2}$$

$$\hat{i}\hat{j} = -\hat{j}\hat{i} = \hat{k},\ \hat{j}\hat{k} = -\hat{k}\hat{j} = \hat{i},\ \hat{k}\hat{i} = -\hat{i}\hat{k} = \hat{j}. \tag{3}$$

A quaternion is divided into a real part (scalar part) and an imaginary part (vector part). The imaginary part has a vector property, where the imaginary numbers behave as unit base vectors, but also have a hypercomplex number property. To assign three-phase AC voltages or currents to the vector part, consider the exponential representation of the quaternion:

$$\boldsymbol{q} = a + \hat{n}||\hat{v}|| = ||\boldsymbol{q}||(\cos\theta + \hat{n}\sin\theta) = ||\boldsymbol{q}||\epsilon^{\hat{n}\theta}, \tag{4}$$

$$\hat{n} = (\hat{i}v_{\rm x} + \hat{j}v_{\rm y} + \hat{k}v_{\rm z})/||\hat{v}||, \tag{5}$$

$$||\boldsymbol{q}||^2 = a^2 + ||\hat{v}||^2, \tag{6}$$

$$||\hat{v}||^2 = (v_{\rm x})^2 + (v_{\rm y})^2 + (v_{\rm z})^2. \tag{7}$$

Let us assign three-phase AC phase (line-to-neutral) voltages to the vector part of the quaternion:

$$\begin{aligned}\boldsymbol{e} =&\ \sqrt{2}E\left\{\begin{matrix}+\hat{i}\cos(\omega t - 0\pi/3) + \hat{j}\cos(\omega t - 2\pi/3)\\ +\hat{k}\cos(\omega t - 4\pi/3)\end{matrix}\right\},\\ =&\ \epsilon^{\hat{n}\omega t}\sqrt{3}E\boldsymbol{e}_0,\end{aligned} \tag{8}$$

$$\hat{n} = (+\hat{i} + \hat{j} + \hat{k})/\sqrt{3}, \tag{9}$$

$$\boldsymbol{e}_0 = \left\{\begin{matrix}+\hat{i}\cos(-0\pi/3) + \hat{j}\cos(-2\pi/3)\\ +\hat{k}\cos(-4\pi/3)\end{matrix}\right\}\Bigg/\sqrt{\frac{3}{2}}. \tag{10}$$

The exponential form of the equation (8) denotes that the initial three-phase (positive phase) AC voltage vector rotates counterclockwise with unit vector axis $\hat{n}$. In this case, the locus of the rotating vector is a circle on the plane, which is perpendicular to $\hat{n}$ and includes the origin.

Next, let us consider Ohm's law of the three-phase AC circuit, where the load is inductive, and the mutual inductances exist as follows:

$$\begin{aligned}\begin{bmatrix}e_{\rm a}\\ e_{\rm b}\\ e_{\rm c}\end{bmatrix} =&\ \sqrt{2}E\begin{bmatrix}\cos(\omega t + \phi - 0\pi/3)\\ \cos(\omega t + \phi - 2\pi/3)\\ \cos(\omega t + \phi - 4\pi/3)\end{bmatrix},\\ =&\ \begin{bmatrix}L + L_{\rm N} & M + L_{\rm N} & M + L_{\rm N}\\ M + L_{\rm N} & L + L_{\rm N} & M + L_{\rm N}\\ M + L_{\rm N} & M + L_{\rm N} & L + L_{\rm N}\end{bmatrix}\\ &\cdot p\sqrt{2}I\begin{bmatrix}\cos(\omega t - 0\pi/3)\\ \cos(\omega t - 2\pi/3)\\ \cos(\omega t - 4\pi/3)\end{bmatrix},\end{aligned} \tag{11}$$

where $p\,(= {\rm d}/{\rm d}t)$ is a differential operator. Because the neutral inductance (grounding inductance) does not affect symmetrical (positive phase) AC, the quaternion representation is as follows [4]:

$$\begin{aligned}\boldsymbol{e} =&\ \epsilon^{\hat{n}(\omega t + \phi)}\sqrt{3}E\boldsymbol{e}_0 = (L - M)p\,\boldsymbol{i},\\ =&\ (L - M)p\,\epsilon^{\hat{n}\omega t}\sqrt{3}I\boldsymbol{i}_0 = \hat{n}\omega(L - M)\,\boldsymbol{i},\end{aligned} \tag{12}$$

where the phase ϕ is $\pi/2$. Three-phase current can be expressed in the exponential form of a quaternion. The quaternion can be easily differentiated in time. Thus, the reactance of an inductance, L, can be simply expressed as $\hat{n}\omega L$.

Consequently, the quaternion representation of general Ohm's law can be presented as follows:

$$[R][\boldsymbol{i}] + [L]\frac{\rm d}{{\rm d}t}[\boldsymbol{i}] = [\boldsymbol{e}], \tag{13}$$

$$\begin{aligned}\boldsymbol{e} =&\ \epsilon^{\hat{n}\omega t}\sqrt{3}E\boldsymbol{e}_0 = \{R + (L - M)p\}\,\boldsymbol{i},\\ =&\ \{R + (L - M)p\}\,\epsilon^{\hat{n}\omega t}\sqrt{3}I\boldsymbol{i}_0,\\ =&\ \{R + \hat{n}\omega(L - M)\}\,\boldsymbol{i}.\end{aligned} \tag{14}$$

When the initial current quaternion is zero (origin), the quaternion spirally approaches the final steady-state circular locus as follows:

$$\boldsymbol{i} = \frac{1}{|Z|\epsilon^{\hat{n}\phi}}\left(\epsilon^{\hat{n}\omega t} - \epsilon^{-t/\tau}\right)\sqrt{3}E\boldsymbol{e}_0, \tag{15}$$

$$Z = R + \hat{n}\omega(L - M) = |Z|\epsilon^{\hat{n}\phi}, \tag{16}$$

$$\tau = (L - M)/R. \tag{17}$$

The equation for the generator is as follows:

$$\begin{bmatrix}V_0\\ V_1\\ V_2\end{bmatrix} = \begin{bmatrix}0\\ E_{\rm a}\\ 0\end{bmatrix} - \begin{bmatrix}Z_0I_0\\ Z_1I_1\\ Z_2I_2\end{bmatrix}. \tag{18}$$

The biquaternion (a usual complex number h independent from the quaternion $\hat{i}, \hat{j}, \hat{k}$) representation is obtained as follows [5]:

$$\sqrt{2}\boldsymbol{V}_0 = 0 - \{R + h\omega(L - M)\}\sqrt{2}\boldsymbol{I}_0, \tag{19}$$

$$\sqrt{2}\boldsymbol{V}_1 = \sqrt{2}\boldsymbol{E}_a - \{R + \hat{n}\omega(L - M)\}\sqrt{2}\boldsymbol{I}_1, \tag{20}$$

$$\sqrt{2}\boldsymbol{V}_2 = 0 - \{R - \hat{n}\omega(L - M)\}\sqrt{2}\boldsymbol{I}_2. \tag{21}$$

The direction $I_0//\hat{n}$ is worthy of attention. Zero-phase AC does not rotate but does oscillate along $\hat{n}$. The sign of $\hat{n}\omega$ is also worthy of attention. The sign of the inductive reactance is minus in the negative phase equation (21).

With quaternion, complex power is expressed as follows (the asterisk symbol in a superfix indicates the complex conjugate of the quaternion).

$$\begin{aligned}\hat{v}\hat{i}^* =&\ (\hat{i}v_{\rm a} + \hat{j}v_{\rm b} + \hat{k}v_{\rm c})(\hat{i}i_{\rm a} + \hat{j}i_{\rm b} + \hat{k}i_{\rm c})^*\\ =&\ (v_{\rm a}i_{\rm a} + v_{\rm b}i_{\rm b} + v_{\rm c}i_{\rm c}) - \hat{i}(v_{\rm b}i_{\rm c} - v_{\rm c}i_{\rm b})\\ &- \hat{j}(v_{\rm c}i_{\rm a} - v_{\rm a}i_{\rm c}) - \hat{k}(v_{\rm a}i_{\rm b} - v_{\rm b}i_{\rm a}).\end{aligned} \tag{22}$$

Concerning the product of the vector parts of quaternions, the scalar part refers to the inner (scalar) product and the vector part refers to the outer (vector) product. Namely, concerning quaternion power, the scalar part represents the active power of three-phase (positive phase) and the vector part represents the reactive power [6]. In the case of an induction motor, the accelerating torque can be obtained from the scalar part, since the active power is the output mechanical power [7]. In the case of a synchronous generator, the decelerating torque can be obtained from the vector part, since the vector product of magnetic flux and current is the electromagnetic force.

3. Motion Equation of the Motor Generator

Here, a motion equation of the motor generator is deduced under the condition that the rotor is a rigid body [8]. According to Newton's Law, the motion of a rigid body is analyzed by dividing it into translational and rotational motions around a gravitational center. The rotational motion is considered in the case of a motor generator. First, a rotational matrix R is adopted to express the orientation of the rigid body. R is interpreted to be a matrix with column vectors that are the direction cosine ones of a unit vector fixed at the rotor in the coodinates (q-axis, d-axis, rotational axis). The differential equation of R is as follows:

$$\frac{\mathrm{d}R}{\mathrm{d}t} = \omega \times R, \tag{23}$$

where ω is the angular velocity vector. When the q-axis (x-axis) rotates counterclockwise around the rotational axis (z-axis), the q-axis (x-axis) becomes located in the direction of d-axis (y-axis).

The differential equation of ω is as follows:

$$\frac{\mathrm{d}}{\mathrm{d}t}(I\omega) = T, \tag{24}$$

where I is the inertia tensor and $I\omega$ is the angular momentum vector. T is the torque vector, which includes the accelerating torque T_A from the induction motor and the decelerating torque T_M from the synchronous generator.

In the equation (23), the matrix expansion method is adopted for the vector product of ω and R:

$$\begin{aligned}\frac{\mathrm{d}R}{\mathrm{d}t} &= \begin{bmatrix} 0 & -\omega_3 & \omega_2 \\ \omega_3 & 0 & -\omega_1 \\ -\omega_2 & \omega_1 & 0 \end{bmatrix} R \\ &= \overleftrightarrow{\omega} R, \end{aligned}\tag{25}$$

where $\overleftrightarrow{\omega}$ is the angular velocity matrix.

In the equation (24), since the rotor is symmetric rotationally, the inertia tensor becomes diagonal:

$$\frac{\mathrm{d}}{\mathrm{d}t}\begin{bmatrix} I_1 & 0 & 0 \\ 0 & I_2 & 0 \\ 0 & 0 & I_3 \end{bmatrix}\begin{bmatrix} \omega_1 \\ \omega_2 \\ \omega_3 \end{bmatrix} = \begin{bmatrix} T_1 \\ T_2 \\ T_3 \end{bmatrix}. \tag{26}$$

Next, a rotational quaternion is considered to express the orientation of the rigid body rotating around only one axis:

$$\boldsymbol{Q} = \exp\left(\frac{\hat{\omega}}{|\hat{\omega}|}\theta\right). \tag{27}$$

The rotational quaternion is interpreted as a quaternion, which rotates by θ counterclockwise around the unit vector $\hat{\omega}/|\hat{\omega}|$. The differential equation of Q is as follows [9]:

$$\begin{aligned}\frac{\mathrm{d}\boldsymbol{Q}}{\mathrm{d}t} &= \frac{\hat{\omega}}{|\hat{\omega}|}\frac{\mathrm{d}\theta}{\mathrm{d}t}\exp\left(\frac{\hat{\omega}}{|\hat{\omega}|}\theta\right) \\ &= \frac{\hat{\omega}}{|\hat{\omega}|}|\hat{\omega}|\boldsymbol{Q} \\ &= \hat{\omega}\boldsymbol{Q}. \end{aligned}\tag{28}$$

Similarity of the product form with the equation (23) or (25) is noticeable. Note that the angular velocity vector $\hat{\omega}$ is the vector part of the angular velocity quaternion ($\hat{\omega} = \hat{i}\omega_1 + \hat{j}\omega_2 + \hat{k}\omega_3$). Although the decelerating torque appears due to the exciting current when the field current is driven, simulation of the load current is executed neglecting the exciting current. The initial state is assumed to be steady state, where the motor generator outputs no-load voltage at the maximum speed [10–12].

$$\begin{aligned}\frac{\mathrm{d}(\omega/\omega_0)}{\mathrm{d}t} &= \frac{1}{\tau_\mathrm{A}}\frac{(r_1 + r_2)(r_2/s)}{(r_1 + r_2/s)^2 + (x_1 + x_2)^2} \\ &\quad - \frac{1}{\tau_\mathrm{G}}\frac{X_\mathrm{a} I_\mathrm{a} E_\mathrm{g}\cos\alpha}{(\omega/\omega_0)V_0^2} - \frac{1}{\tau_\mathrm{M}}, \end{aligned}\tag{29}$$

$$\frac{1}{\tau_\mathrm{A}} = \frac{3V_0^2}{I\omega_0^2(r_1 + r_2)}, \tag{30}$$

$$\frac{1}{\tau_\mathrm{G}} = \frac{3V_0^2}{I\omega_0^2 X_\mathrm{a}}, \tag{31}$$

$$\frac{1}{\tau_\mathrm{M}} = \frac{T_\mathrm{M}}{I\omega_0}, \tag{32}$$

$$s = \frac{\omega_0 - \omega}{\omega_0} = 1 - (\omega/\omega_0), \tag{33}$$

where τ_A is the time constant for acceleration by an induction motor, τ_G is that for deceleration by a synchronous generator, τ_M is that for deceleration by mechanical loss and windage loss, X_a is synchronous reactance, I_a is armature current, E_g is armature output voltage, ω_0 is the synchronous speed of the induction motor, V_0 is the rated output voltage of the synchronous generator and T_M is the torque for deceleration by mechanical loss and windage loss. α is the power factor angle of the load, which is the phase angle of the thyristor power supply.

Time evolutions of acceleration from the start to the waiting speed, acceleration to the maximum speed, and

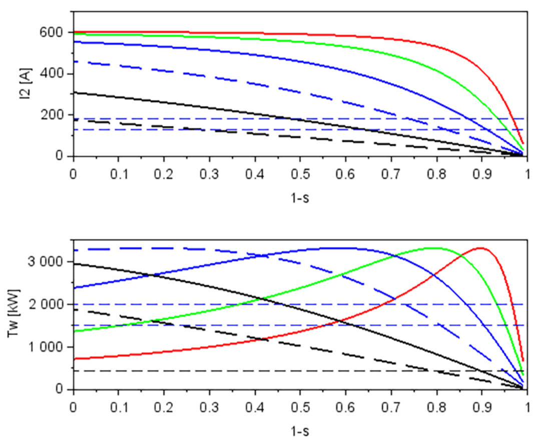

Fig. 1 Slip dependence of secondary current and synchronous watt in an induction motor. Secondary resistance is r_2 (red), $2 * r_2$ (green), $4 * r_2$ (blue), $8 * r_2$ (dot-dashed blue), $16 * r_2$ (black), and $32 * r_2$ (dot-dashed black) by adding a liquid resistance to the original r_2 in series. Ordinate of abscissa is scaled by not s (slip) but $1 - s$.

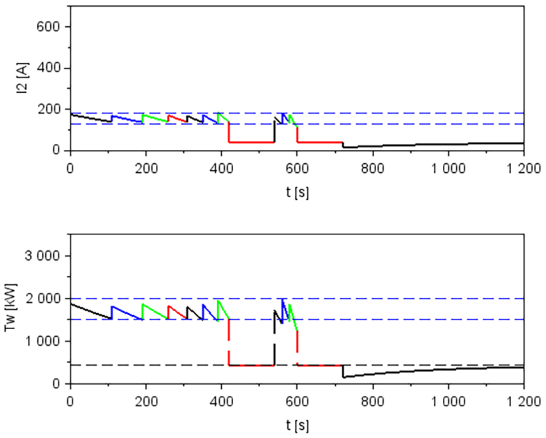

Fig. 2 Time evolution of secondary current and synchronous watt (synchronous angular velocity times torque) in an induction motor. Secondary resistance is adjusted so as to keep the armature current below the maximum current (blue dashed line) by adjusting the liquid resistance connected to the original r_2 in series.

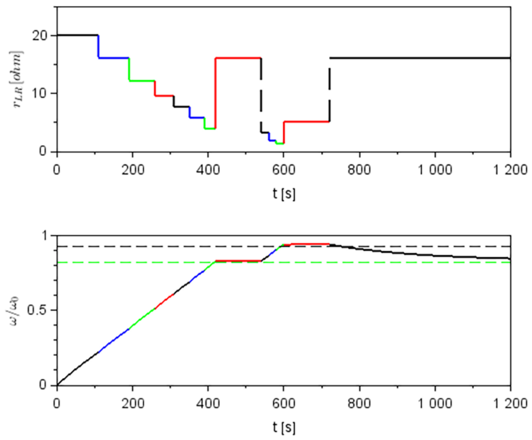

Fig. 3 Time evolution of the liquid resistance and rotating speed normalized by the synchronous speed in the accelerating stage toward the waiting speed, from it toward the maximum speed, and in the free-running stage toward the waiting speed. Secondary resistance is adjusted so as to keep the armature current below the maximum current by adjusting the liquid resistance connected to the original r_2 in series.

deceleration to the waiting speed are shown by keeping the induction motor current below the endurable maximum current (Figs. 1, 2, 3). In the state of maximum speed, exciting current is driven and no-load induced voltage is output. If the output current is supplied to the power supply of the poloidal field coil, the motor-generator is decelerated by electromagnetic force due to the current.

4. Transient Phenomena in Motor-Generator

In the case of a salient type, the armature current I_a is divided into direct and quadrature components:

$$I_a = -jI_d + I_q. \tag{34}$$

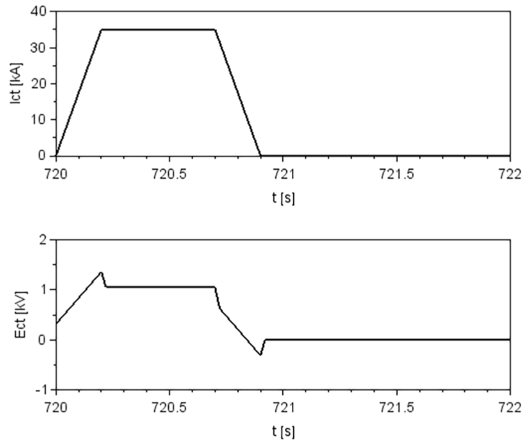

Fig. 4 Time evolution of poloidal field coil current and voltage. The flat-top current is assumed to be 35 kA to emphasize the effect on the motor-generator. The inductance and resistance of the coil are L = 1.8 mH and R = 30 mΩ, respectively.

Adopting the direct reactance as X_d and the quadrature one as X_q, the output voltage of synchronous generator is:

$$\begin{aligned} E_f - E_g &= (+jX_d)(-jI_d) + (+jX_q)(I_q) \\ &= X_d I_d + jX_q I_q, \end{aligned} \tag{35}$$

where E_f is the no-load output voltage and E_g is output terminal voltage. Since $X_d > X_q$, the armature reaction dropped due to fact that the smaller quadrature reactance in a salient type is lower than that due to the direct reactance in a non-salient type. Even if three-phase AC is assigned to the vector part of the quaternion, an imaginary number j has only to replace $\hat{n}$ in the equation (35).

$$\begin{aligned} \boldsymbol{E}_f - \boldsymbol{E}_g &= (+\hat{n}X_d)(-\hat{n}\boldsymbol{I}_d) + (+\hat{n}X_q)(\boldsymbol{I}_q) \\ &= -\hat{n}^2 X_d \boldsymbol{I}_d + \hat{n}X_q\boldsymbol{I}_q = X_d\boldsymbol{I}_d + \hat{n}X_q\boldsymbol{I}_q, \end{aligned} \tag{36}$$

where $\boldsymbol{E}_f$, $\boldsymbol{E}_g$, $\boldsymbol{I}_d$ and $\boldsymbol{I}_q$ are quaternions though the same variables are used.

When time evolution on the DC side of the power supply for the poloidal field is given:

$$E = L\frac{dI}{dt} + RI, \tag{37}$$

$$I_a = \sqrt{\frac{2}{3}}I, \tag{38}$$

$$E_g \cos\alpha = \frac{\pi}{3\sqrt{2}}E, \tag{39}$$

$$E_g \sin\alpha = \sqrt{(E_f)^2 - (E_g\cos\alpha)^2} - X_a I_a, \tag{40}$$

$$E_g = \sqrt{(E_g\cos\alpha)^2 + (E_g\sin\alpha)^2}. \tag{41}$$

The current waveform of the power supply shown in Fig. 4 is considered.

In the phase where the output current is flat in time, the field current is controlled so as to keep the output voltage within the rated output voltage range. In the case of the integral time constant equal to 0.5 s, waveforms of field current and output voltage are shown (Fig. 5). The output voltage approaches the rated voltage in the flat phase of the output current.

Field current is adjusted by PI-controlling the field voltage so that the generator output voltage becomes equal to the rated voltage. The differential equation is as follows:

$$\tau_f \frac{d}{dt}\frac{(I_f - I_{fref})}{I_{fref}} + \frac{(I_f - I_{fref})}{I_{fref}} = G_P\left(\frac{(E_{gref} - E_g)}{E_{gref}} + \frac{(E_{gref} - E_g)}{E_{gref}(1 + s\tau_I)}\right), \quad (42)$$

where E_{gref} and I_{fref} are rated output phase voltage and necessary field current, respectively. τ_f and τ_I are the time constants of the field coil and integral control, respectively, and G_P is the gain for proportional control. In the integral control, not a complete integral but a first-order-lag integral is adopted. Though the first-order-lag integral is expressed in Laplace transform format, the following differential equations are solved by computer simulation:

$$\tau_f \frac{d}{dt}\frac{(I_f - I_{fref})}{I_{fref}} + \frac{(I_f - I_{fref})}{I_{fref}} = G_P\left(\frac{(E_{gref} - E_g)}{E_{gref}} + E_{gI}\right), \quad (43)$$

$$\tau_I \frac{dE_{gI}}{dt} + E_{gI} = \frac{(E_{gref} - E_g)}{E_{gref}}. \quad (44)$$

When the output voltage of the synchronous generator changes, the firing angle is adjusted so that the coil current approaches the reference value in the power supply for the poloidal field (PF) coil. The firing angle is obtained if the control equation is solved by the computer simulation.

$$(L/R)\frac{d\alpha}{dt} + \alpha = \frac{R}{E^{PF}_{ref}} G^{PF}_P\left((I - I^{PF}_{ref}) + \frac{(I - I^{PF}_{ref})}{(1 + s\tau^{PF}_I)}\right), \quad (45)$$

$$L\frac{dI}{dt} + RI = E_g \frac{3\sqrt{6}}{\pi}\cos\alpha, \quad (46)$$

where I^{PF}_{ref} is the control reference value of the output current from the power supply for the PF coil.

The equations to solve (E_g, δ_1) via (I_q, I_d) from (I_a, α, E_f) are as follows:

$$I_a \sin(\alpha + \delta_1) = I_d, \quad (47)$$

$$I_a \cos(\alpha + \delta_1) = I_q, \quad (48)$$

$$E_g \sin\delta_1 = X_q I_q, \quad (49)$$

$$E_g \cos\delta_1 = E_f - X_d I_d, \quad (50)$$

δ_1 dependence of E_{g1} is determined from the direct component of equations (47) and (50), and the dependence of E_{g2} is determined from the quadrature component of equations (48) and (49), which are shown in Fig. 6. The values of E_g and δ_1 are obtained from the intersection of both lines.

Simulation results of generator output induced voltage and output terminal voltage are shown (Fig. 7). Control of output induced voltage is not smoothly controlled. This is because the claculation of δ_1 is not correct when the controlled firing phase angle is over 90 degrees. Cooperation is necessary between phase control in the power supply of the poloidal field coil and current control in the field coil.

Since the armature reactance is relatively large, output voltage control is difficult when the output current is low. Since the exciting current flows in the load transformer, a low output curent region can be prevented by driving the current. When the power factor is low in the load of the generator, the induced voltage must be large. When the load power supply is operated in the regenerative mode,

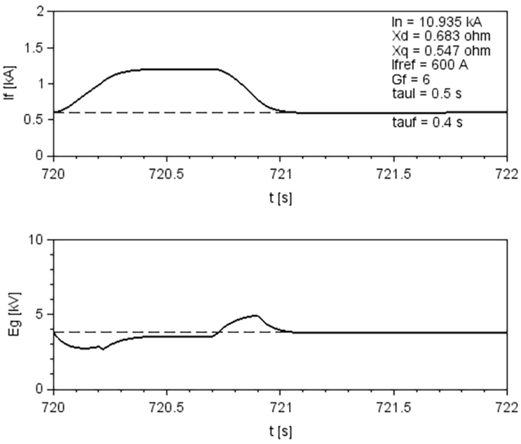

Fig. 5 Time evolution of field current and output voltage of a synchronous generator. The field current is feedback-controlled so as to keep the output terminal voltage constant where the proportional gain is six, the integral time constant is 0.5 s, and the first-order-delay time constant is 0.4 s.

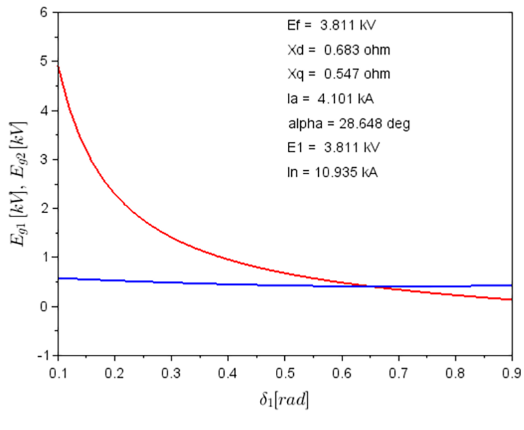

Fig. 6 Dependence of output terminal voltage E_g on angle of phase difference δ_1 is shown for the direct-axis component (red) and the quadrature-axis component (blue). The output current of the synchronous generator is 3/8 of the rated current.

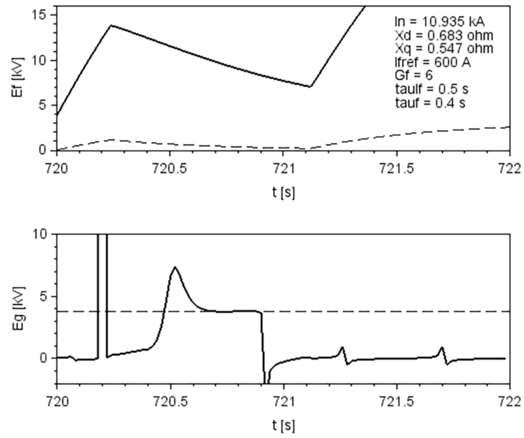

Fig. 7 Time evolutions of generator output induced voltage E_f and output terminal voltage E_g are shown.

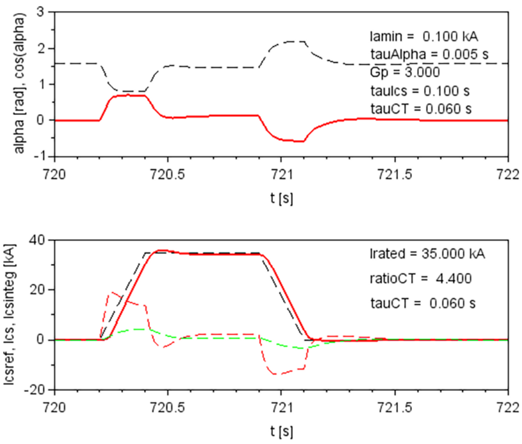

Fig. 8 Time evolutions of controlled phase angle α (black dashed), $\cos\alpha$ (red), and I_{CS} are shown. I_{CS}: I_{csref} (black dashed), P-controlled I_{cspro} (green dashed), I-controlled $I_{csinteg}$ (red dashed) and totally controlled I_{cs} (red solid).

the output terminal voltage cannot be determined stably. Namely, there is a gap between the power mode and the regenerative mode.

Simulation result after optimization of control parameters in the power supply is shown in Fig. 8. In the phase control of the firing angle (black broken line), the proportional gain increased and the integral time constant decreased. Together with the current waveform (red solid line), the P-controlled part is shown in a red broken line and the I-controlled part is shown in a dash dotted line. In the current waveform (red solid line), time delay from the reference waveform (black broken line) decreases and the difference from it to the flat top also decreases.

5. Summary

In the transient phase at the start of the induction motor, high transient current flows in the stator coil. By setting the liquid resistance to the maximum value, high current is prevented, and the rotation speed is controlled by adjusting the liquid resistance value.

In the transient phase at the start of the synchronous generator, high transient voltage appears in the armature windings repeatedly. Due to the repeatability, it is imperative to estimate the high voltage and control it so that the maximum voltage is kept under the tolerable value.

Utilizing the quaternion capability, the three-phase motor-generator is analyzed by three-dimensional rotation instead of by transforming to two-dimensional rotation in alpha-beta coordinates [1]. Although the mechanical rotation can be analyzed by rotation quaternion instead of by rotation matrix, its usage was abandoned because the vibration of the rotation axis was not analyzed. The salient pole-type rotating field can be manipulated by direct-quadrature conversion even in quaternion analysis. Since the quadrature reactance is lower than the direct reactance, consideration of the same did not worsen the simulation result.

The rotating dynamics and electrical phenomena of a motor-generator can be analyzed considering the quaternion power from the motor-generator and the electrical load for plasma control. Since the quaternion can be differentiated in time as well as rotated in space [2], it was utilized to analyze transient phenomena in the rise-up and rise-down of the induction motor and the synchronous generator. Since the armature reactance is relatively large, output voltage control was difficult when the output current was low. Since the exciting current flows in the load transformer, the low output current region should be prevented by driving the current.

When the power factor is low in the load of the generator, the induced voltage must be large. When the load power supply is operated in the regenerative mode, the output terminal voltage could not be determined stably. Namely, there was a gap between the power mode and the regenerative mode. The quaternion characteristics will be utilized to analyze a motor-generator in more detail.

Acknowledgment

This work was performed partly with the support and under the auspices of the NIFS Collaboration Research program (NIFS22KUTR165, NIFS22KIEA012).

[1] K. Nakamura, Y. Zhang, T. Onchi, H. Idei, M. Hasegawa, K. Tokunaga, K. Hanada, O. Mitarai, S. Kawasaki, A. Higashijima, T. Nagata and S. Shimabukuro, Quaternion Analysis of a Direct Matrix Converter Based on Space-Vector Modulation, Plasma Fusion Res. **16**, 2405037 (2021).

[2] K. Nakamura, Y. Zhang, T. Onchi, H. Idei, M. Hasegawa, K. Tokunaga, K. Hanada, H. Chikaraishi, O. Mitarai, S. Kawasaki, A. Higashijima, T. Nagata and S. Shimabukuro, Quaternion Analysis of Transient Phenomena in Matrix Converter Based on Space-Vector Modulation, Plasma Fusion Res. **17**, 2405025 (2022).

[3] P. Kellan and P.G. Tait, *Introduction to Quaternions* (MacMillan and Co., Limited, 1904).

[4] K. Nakamura, I. Jamil, X.L. Liu, O. Mitarai, M. Hasegawa,

K. Tokunaga, K. Araki, H. Zushi, K. Hanada, A. Fujisawa, H. Idei, Y. Nagashima, S. Kawasaki, H. Nakashima and A. Higashijima, Quaternion Analysis of Three-Phase Power Electronic Circuit by Using Conjugation, International Conference on Electrical Engineering, ICEE 2015, 15A-476 (2015).

[5] K. Nakamura, M. Hasegawa, K. Tokunaga, K. Araki, I. Jamil, X.L. Liu, O. Mitarai, H. Zushi, K. Hanada, A. Fujisawa, H. Idei, Y. Nagashima, S. Kawasaki, H. Nakashima, A. Higashijima and T. Nagata, Quaternion Analysis of Three-Phase Matrix Converter Switching Method, International Conference on Electrical Engineering, ICEE 2016, D2-4: id 90432 (2016).

[6] H. Akagi, Y. Kanazawa, K. Fugita and A. Nanba, Generalized Theory of the Instantaneous Reactive Power and its Application, Trans. IEE of Japan, **103-B**, 7, 483 (1983).

[7] J.H. Conway and D. Smith, *On Quaternions and Octonions: Their Geometry, Arithmetic, and Symmetry* (A.K. Perters, Ltd, 2003).

[8] E. Lengyel, *Mathematics for 3D Game Programming and Computer Graphics, 3rd Edition* (Charles River Media, Inc., 2001).

[9] J. Vince, *Rotation Transforms for Computer Graphics* (Springer-Verlag, 2011).

[10] F.T. Chapman, *A Study of the Induction Motor* (Chapman & Hall, 1930).

[11] T. Torda, *Design of Alternating Generators and Synchronous Motors* (McGraw Publishing Company, 1908).

[12] R.E. Brown, *Alternating-Current Machinery: a Text-Book on the Theory and Performance of Generators and Motors* (John Wiley, 1927).